THE JOURNAL OF PHYSICAL CHEMISTRY A

Article

pubs.acs.org/JPCA

Computational Study of Chain Transfer to Monomer Reactions in High-Temperature Polymerization of Alkyl Acrylates

Nazanin Moghadam,[†] Shi Liu,[‡] Sriraj Srinivasan,[§] Michael C. Grady,[∥] Masoud Soroush,*[,†] and Andrew M. Rappe[‡]

[†]Department of Chemical and Biological Engineering, Drexel University, Philadelphia, Pennsylvania 19104, United States

[‡]The Makineni Theoretical Laboratories, Department of Chemistry, University of Pennsylvania, Philadelphia, Pennsylvania 19104-6323, United States

[§]Arkema Inc., 900 First Avenue, King of Prussia, Pennsylvania 19406, United States

[∥]DuPont Experimental Station, Wilmington, Delaware 19898, United States

Supporting Information

ABSTRACT: This article presents a computational study of chain transfer to monomer (CTM) reactions in self-initiated high-temperature homopolymerization of alkyl acrylates (methyl, ethyl, and *n*-butyl acrylate). Several mechanisms of CTM are studied. The effects of the length of live polymer chains and the type of monoradical that initiated the live polymer chains on the energy barriers and rate constants of the involved reaction steps are investigated theoretically. All calculations are carried out using density functional theory. Three types of hybrid functionals (B3LYP, X3LYP, and M06-2X) and four basis sets (6-31G(d), 6-31G(d,p), 6-311G(d), and 6-311G(d,p)) are applied to predict the molecular geometries of the reactants, products and transition sates, and energy barriers. Transition state theory is used to estimate rate constants. The results indicate that abstraction of a hydrogen atom (by live polymer chains) from the methyl group in methyl acrylate, the methylene group in ethyl acrylate, and methylene groups in *n*-butyl acrylate are the most likely mechanisms of CTM. Also, the rate constants of CTM reactions calculated using M06-2X are in good agreement with those estimated from polymer sample measurements using macroscopic mechanistic models. The rate constant values do not change significantly with the length of live polymer chains. Abstraction of a hydrogen atom by a tertiary radical has a higher energy barrier than abstraction by a secondary radical, which agrees with experimental findings. The calculated and experimental NMR spectra of dead polymer chains produced by CTM reactions are comparable. This theoretical/computational study reveals that CTM occurs most likely via hydrogen abstraction by live polymer chains from the methyl group of methyl acrylate and methylene group(s) of ethyl (*n*-butyl) acrylate.

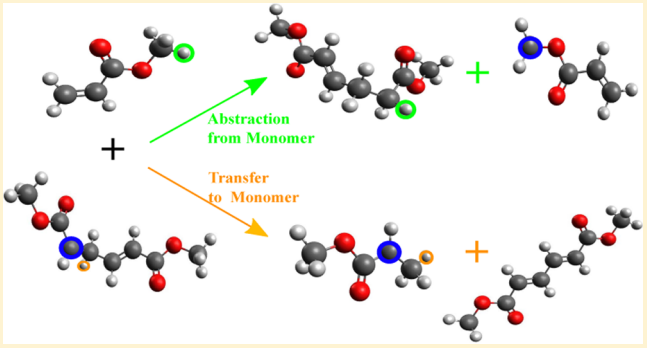

1. INTRODUCTION

Acrylic resins are thermoplastic polymers that are widely used in the development of automotive paint and coatings, adhesives, and functional additives.[1−5] The basic nature of acrylic resins and the plants producing the resins have changed considerably over the past decades as a result of environmental limits on allowable volatile organic contents (VOCs) of resins.[6−8] High temperature (>100 °C) polymerization, which allows for the production of high-solids low-molecular-weight resins, has mostly replaced conventional (low-temperature) polymerization, which produces low-solids high-molecular-weight resins.[1,9,10] It was reported[1,2,11−15] that, at the high temperatures, secondary reactions, such as spontaneous initiation (in the absence of known added initiators), chain transfer to monomer and polymer, backbiting, and β-scission reactions, occur at higher rates in polymerization of alkyl acrylates. The polydispersity index, which is a measure of the breadth of the polymer chain length distribution, was found to be 1.5 to 2.2[14,16] in high-temperature homopolymerization of alkyl acrylates. Recent studies using quantum chemical calculations[11,12] and matrix-assisted laser desorption ionization (MALDI)[16] showed that monomer self-initiation is a likely mechanism of initiation in spontaneous thermal polymerization of alkyl acrylates. The monoradicals generated by self-initiation[11,12] are shown in Figure 1.

Previous studies of self-initiated polymerization of methyl acrylate (MA), ethyl acrylate (EA), and *n*-butyl acrylate (*n*-BA) using electro-spray ionization−Fourier transform mass spectrometry (ESI-FTMS)[14] and MALDI[16] showed abundant polymer chains with end-groups formed by chain transfer

Received: October 11, 2012
Revised: February 4, 2013
Published: February 13, 2013

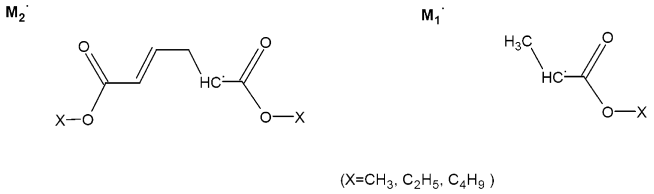

Figure 1. Two types of monoradical generated by self-initiation.[12]

reactions. Nuclear magnetic resonance (NMR) analysis of these polymers indicates the possible presence of end groups from chain-transfer-to-monomer (CTM) reactions at various temperatures (100−180 °C).[14] CTM reactions are capable of limiting the maximum polymer molecular weight that can be achieved for a given monomer[17,18] and strongly influence the molecular weight distribution of dead polymer chains.[19−22] These suggest that a better understanding of mechanisms of CTM is important for developing more efficient high-temperature polymerization processes.

Controlled radical polymerization processes, such as nitroxide-mediated polymerization (NMP), atom transfer radical polymerization (ATRP), and reversible addition−fragmentation chain transfer (RAFT), involve the use of agents to control the growth of propagating chains, which leads to the formation of uniform chain-length polymers.[23−29] It has been reported that, in thermal polymerization of alkyl acrylates, in the absence of these agents, self-regulation and consequently uniform chain length polymers can be achieved.[30] These suggest that some of the chain transfer mechanisms are capable of being self-regulatory. Therefore, a good understanding of the underlying mechanisms is needed to develop controlled thermal polymerization processes. To the best of our knowledge, this work is the first study of all likely mechanisms of CTM in three alkyl acrylates (MA, EA, and *n*-BA), revealing the most likely CTM mechanisms in the homopolymerization. Before this study, only a general description of a chain transfer reaction was available as a reaction of a live polymer chain with a transfer agent (monomer, polymer, solvent, or initiator), without providing any reaction mechanisms.[31,32]

Pulsed-laser polymerization/size exclusion chromatography (PLP/SEC) experiments were carried out at low and high temperatures for determination of chain transfer and radical propagation rate coefficients of acrylates.[33−35] While reliable rate constants and narrow polymer molecular weight distribution were obtained at less than 30 °C, broad molecular-weight distribution and inaccurate rate constants were reported at temperatures above 30 °C.[36−38] Chain transfer to monomer[33,34,36] and to polymer (specifically backbiting)[37,39,40] were identified as the main reactions that were causing the discrepancies in the molecular-weight distributions and reaction rate coefficients.

Reaction rate constants in high-temperature polymerization of alkyl acrylates have typically been estimated from polymer sample measurements such as monomer conversion and average molecular weights. The measured monomer conversion and molecular weights have been fitted to a macroscopic mechanistic model to determine the kinetics of polymerization.[2,41,42] The rate constants of CTM reactions in methyl methacrylate (MMA), styrene, and α-methylstyrene polymerization have been determined with little difficulty.[20] Gilbert et al.[22] estimated rate constants of CTM reactions in emulsion polymerization of *n*-BA from polymer molecular weight distributions. Previous reports have shown that hydrogen abstraction by tertiary poly-*n*-BA live chains contributes to the rate of CTM.[19,43,44] However, the reliability of the estimated rate coefficients is dependent on the validity of the postulated reaction mechanisms and the certainty of the measurements. Because of these concerns, macroscopic mechanistic modeling is sometimes incapable of determining either the reaction mechanisms or the individual reaction step rates conclusively.

Previous reports showed that hydrogen abstraction by tertiary poly-*n*-BA live chains contributes to the rate of CTM.[19,43,44] However, CTM rate constants for free-radical polymerization of acrylates have been reported to be difficult to estimate due to large uncertainties in experimental measurements.[43] The presence of trace impurities, which can act as chain transfer agents, was mentioned as the cause for the variation in estimated rate constant values.[22,45,46] The temperature dependence of the rate constant of transfer to monomer reaction in styrene was estimated from polymer sample measurements.[47] Considering the difficulties in estimating CTM rate constants, computational quantum chemistry has been considered as an alternative way of estimating these parameters.

Both density functional theory (DFT) and wave function-based quantum chemical methods have been used to study free-radical polymerization reaction mechanisms such as self-initiation and propagation reactions in thermal polymerization of alkyl acrylates.[11,12,48−51] DFT is, in principle, an exact ground-state technique. The accuracy of DFT depends on the approximation of exchange-correlation functionals. Generally, DFT can predict molecular geometries with high accuracy[52] but energy barriers with less accuracy compared to high-level wave function-based methods such as MP2.[53] It is important to note that modern exchange-correlation functionals such as M06[54] and ωB97x-D[55] have increased the reliability and accuracy of DFT-predicted energy barriers. These functionals have allowed exploration of the molecular and kinetic properties of larger molecules such as polymer chains and chain transfer reactions at lower computational cost and with reasonably good accuracy.[49] For large (greater than 30 atoms) polymer systems, DFT[56] has been shown to be a practical and reliable substitute for wave function-based methods.[57] One should ascertain the adequacy of a level of theory for a system of interest prior to estimating the kinetics and thermodynamics of reaction. Exchange-correlation functionals can be classified based on their functional form.[58−60] Local functionals (depending only on charge density $\rho(\mathbf{r})$ at point $\mathbf{r}$), generalized gradient-approximation (GGA) (depending on $\rho(\mathbf{r})$ and $|\nabla\rho(\mathbf{r})|$), and meta-GGA functionals (depending on $\rho(\mathbf{r})$, $|\nabla\rho(\mathbf{r})|$, and $\nabla^2\rho(\mathbf{r})$) can be combined with Hartree−Fock exchange functionals to increase accuracy. These combined functionals are known as hybrid functionals. B3LYP, which is a hybrid GGA functional, has been used extensively due to its attractive performance-to-cost ratio.[11,12] For example, B3LYP/6-31G(d) has been used to study self-initiation of styrene,[61] MA, EA, *n*-BA,[11,12] and MMA.[48] B3LYP/6-31G(d) was found[42] to underestimate the reaction rate constants for self-initiation of MA in comparison to MP2/6-31G(d). Because of high computational costs and inherent size limitations of MP2/6-31G(d), this level of theory is not used to study chain transfer reactions of large polymer chains. In addition, B3LYP/6-31G(d) has also predicted alkyl acrylate self-initiation rate constants different from those estimated from polymer sample measurements. Meta-GGA and hybrid meta-GGA functionals such as M06-2X provide more accurate prediction of barrier

dx.doi.org/10.1021/jp3100798 | J. Phys. Chem. A 2013, 117, 2605−2618

Scheme 1. Possible End-Chain Transfer to Monomer Reactions of MA (Me=Methyl)

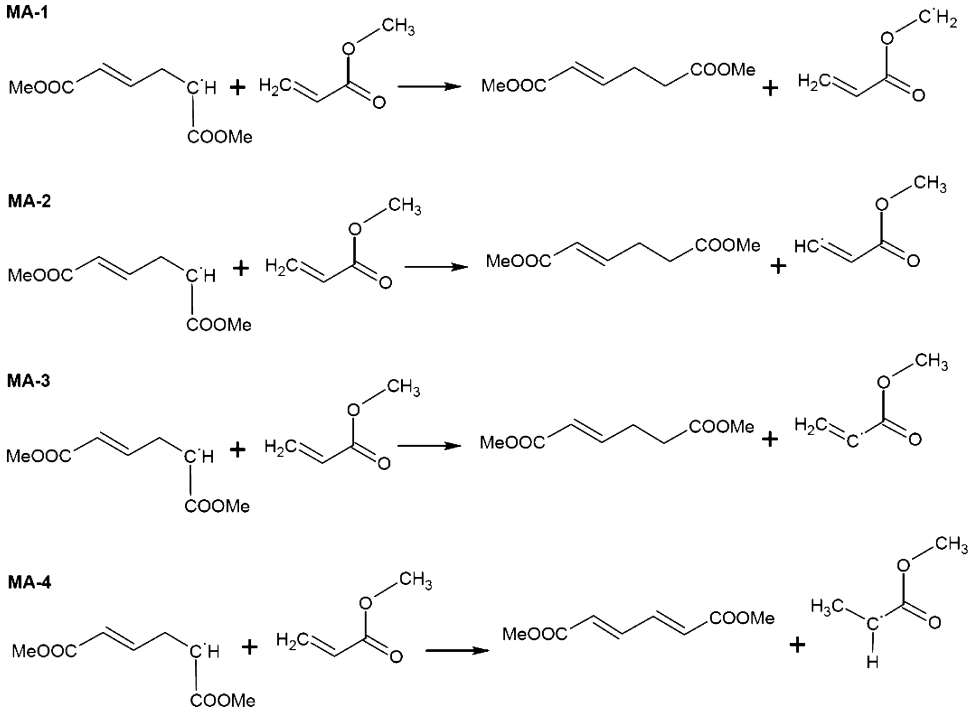

heights, as they can take into account for van der Waals interactions.[54,62−65]

Reports indicate that solvent molecules participate in chain transfer reactions.[66] They tend to act as chain transfer agents by reacting with live polymer chains and, consequently, affecting the microstructure and polydispersity of polymer chains. Experimental studies[16] have shown that the polarity of solvents can impact the rate of initiation reactions in thermal polymerization of alkyl acrylates. Energy barriers predicted using the polarizable continuum model (PCM) and gas phase quantum chemical calculations for polymerization of acrylic acid and acrylates in inert and nonpolar solvents have been found to be similar.[67,68] The use of PCM for polar solvents has been less successful.[69] This may be attributed to the fact that PCM only takes into account electrostatic interactions, while neglecting nonelectrostatic interactions, such as hydrogen bonding and van der Waals interactions. The solvent effect is described better by the hybrid quantum mechanical/molecular mechanical (QM/MM) method, in which a small (more relevant) portion of the system is treated quantum mechanically, and the rest of the system (with explicit solvents) is described by classical force fields.[70,71] The QM/MM method has been applied to study the molecular behavior of proteins.[72] However, the application of QM/MM is limited by the scarcity of accurate MM parameters and the difficulty to describe an accurate QM/MM interface.[70−72] In this study, all calculations are performed in the gas phase to make the computations affordable.

^{13}C NMR has been used to study EA and *n*-BA homopolymerization.[14,73] The peaks assigned to the carbon atoms in different positions along the main chain or the side chain can help determine which molecular structures are formed during the polymerization process. On the basis of these results, one can validate proposed reaction mechanisms. In this work, the NMR spectra of dead polymer chains and end groups have been computed using various levels of theory. We use ORCA program[74] with B3LYP and X3LYP functionals to predict chemical shifts. B3LYP has been reported to be one of the best functionals for ^{1}H chemical shift prediction and provide reasonably accurate ^{13}C chemical shifts.[75] The proposed mechanisms of CTM have been confirmed using the computed NMR spectra.

This article presents a computational investigation of several mechanisms of CTM in self-initiated homopolymerization of MA, EA, and *n*-BA using B3LYP,[76,77] X3LYP, and M06-2X[54,64,65] functionals, and 6-31G(d), 6-31G(d,p), 6-311G(d), and 6-311G(d,p) basis sets. Energy barriers and rate constants of the reactions involved in the postulated mechanisms are estimated. The effect of live polymer chain length, the type of monoradical that initiated the live polymer chain, and the type of live polymer chain radical (tertiary vs secondary) on the kinetics of the CTM reactions are studied.

The organization of the rest of the article is as follows. Section 2 discusses the computational methods applied. Section 3 presents results and discussion. Finally, section 4 presents concluding remarks.

2. COMPUTATIONAL METHODS

All calculations are performed using GAMESS.[78] The functionals B3LYP, X3LYP, and M06-2X with the basis sets 6-31G(d), 6-31G (d,p), 6-311G(d), and 6-311G(d,p) are used to determine the molecular geometries of reactants, products, and transition states in gas phase. Optimized structures are characterized with Hessian calculations. A rate constant $k(T)$ is calculated using transition state theory[79] with

$$k(T) = (c^0)^{1-m}\frac{k_B T}{h}\exp\left(-\frac{\Delta H^{\ddagger} - T\Delta S^{\ddagger}}{RT}\right) \quad (1)$$

where c^0 is the inverse of the reference volume assumed in translational partition function calculation, k_B is the Boltzmann constant, T is temperature, h is Planck's constant, R is the

dx.doi.org/10.1021/jp3100798 | J. Phys. Chem. A 2013, 117, 2605−2618

Table 1. Activation Energy (E_a), Enthalpy of Activation ($\Delta H^{\ddagger}$), and Gibb's Free Energy of Activation ($\Delta G^{\ddagger}$) in kJ mol^{-1}; Frequency Factor (A) and Rate Constant (k) in M^{-1} s^{-1} for the Four CTM Reactions of MA at 298 K

	B3LYP 6-31G(d)	B3LYP 6-31G(d)	B3LYP 6-311G(d)	B3LYP 6-311G(d,p)	X3LYP 6-31G(d,p)	X3LYP 6-311G(d)	X3LYP 6-311G(d,p)	M06-2X 6-31G(d,p)	M06-2X 6-311G(d)	M06-2X 6-311G(d,p)
Hydrogen Abstraction via MA-1										
E_a	71	68	74	71	62	68	65	56	61	58
$\Delta H^{\ddagger}$	66	63	69	66	57	63	60	51	56	54
$\Delta G^{\ddagger}$	114	111	117	114	110	116	113	108	112	110
$\log_e A$	15.4	15.46	15.56	15.5	13.3	13.28	13.36	11.77	11.93	12.07
k	1.8×10^{-06}	5.3×10^{-06}	5.4×10^{-07}	1.8×10^{-06}	9×10^{-06}	7.8×10^{-07}	2.9×10^{-06}	1.7×10^{-05}	3×10^{-06}	8.1×10^{-06}
Hydrogen Abstraction via MA-2										
E_a	100	98	102	100	95	94	95	90	93	92
$\Delta H^{\ddagger}$	95	93	97	95	90	89	90	85	88	87
$\Delta G^{\ddagger}$	137	134	138	137	127	145	137	135	137	134
$\log_e A$	17.6	18.05	18.11	18	19.96	12.42	16	14.34	15	15.47
k	1.5×10^{-10}	5.4×10^{-10}	9.9×10^{-11}	1.7×10^{-10}	9.7×10^{-09}	6.9×10^{-12}	1.7×10^{-10}	3.1×10^{-10}	1.6×10^{-10}	4.2×10^{-10}
Hydrogen Abstraction via MA-3										
E_a	93	91	94	95	87	93	91	80	84	83
$\Delta H^{\ddagger}$	88	86	89	90	82	88	86	75	79	78
$\Delta G^{\ddagger}$	129	127	139	130	122	127	126	125	130	128
$\log_e A$	18.22	18.10	14.72	18.51	18.77	18.95	18.51	14.33	13.95	14.19
k	4.2×10^{-09}	8.3×10^{-09}	7.7×10^{-11}	2.3×10^{-09}	7.6×10^{-08}	1.0×10^{-08}	1.3×10^{-08}	1.7×10^{-08}	2.5×10^{-09}	4.9×10^{-09}
Hydrogen Transfer via MA-4										
E_a	79	75	81	79	73	79	78	73	75	71
$\Delta H^{\ddagger}$	74	70	76	74	68	74	73	68	70	66
$\Delta G^{\ddagger}$	124	118	125	121	116	124	119	120	124	128
$\log_e A$	14.41	15.34	15.2	15.5	15.34	14.37	15.92	13.61	13.07	9.67
k	3.2×10^{-08}	2.9×10^{-07}	2.2×10^{-08}	7.9×10^{-08}	6.8×10^{-07}	2.9×10^{-08}	2.0×10^{-07}	1.6×10^{-07}	2.9×10^{-08}	6.3×10^{-09}

Table 2. H−R Bond Dissociation Energies (kJ mol^{-1}) at 298 K

B3LYP 6-31G(d,p)	B3LYP 6-311G(d)	B3LYP 6-311G(d,p)	X3LYP 6-31G(d,p)	X3LYP 6-311G(d)	X3LYP 6-311G(d,p)
Methyl Hydrogen (MA-1)					
432	425	425	433	426	426
Vinylic Hydrogen (MA-2)					
483	474	478	484	475	479
Methine Hydrogen (MA-3)					
490	480	484	491	482	485
Methylene Hydrogen (EA-1)					
421	414	415	422	415	417
Methyl Hydrogen (EA-2)					
452	443	445	453	445	446
Methylene Hydrogen (*n*-BA-1)					
420	412	413	422	414	416
Methylene Hydrogen (*n*-BA-2)					
433	424	426	435	426	428
Methylene Hydrogen (*n*-BA-3)					
430	421	423	431	423	424
Methyl Hydrogen (*n*-BA-4)					
447	438	440	448	439	441

universal gas constant, m is the molecularity of the reaction, and $\Delta S^{\ddagger}$ and $\Delta H^{\ddagger}$ are the entropy and enthalpy of activation, respectively. $\Delta H^{\ddagger}$ is given by

$$\Delta H^{\ddagger} = (E_0 + ZPVE + \Delta\Delta H)_{TS-R} \quad (2)$$

where $\Delta\Delta H$ is a temperature correction; ZPVE is the difference in zero-point vibrational energy between the transition state and the reactants; and E_0 is the difference in electronic energy of the transition state and the reactants. The activation energy (E_a) is calculated using

$$E_a = \Delta H^{\ddagger} + mRT \quad (3)$$

and the frequency factor (A) by

$$A = (c^0)^{1-m}\frac{k_B T}{h}\exp\left(\frac{mR + \Delta S^{\ddagger}}{R}\right) \quad (4)$$

$\Delta\Delta H$, ZPVE, and $\Delta S^{\ddagger}$ calculations are carried out using the RRHO approximation.[80] This approximation treats the whole molecule as a rigid rotor (RR) and each vibrational mode as a harmonic oscillator (HO). This approximation allows the rotational and vibrational entropies to be calculated separately. It has been shown in previous studies[11,12,48,81] that the RRHO approximation exhibits reasonable computational cost and accuracy for studying large polymer system. Scaling factors of

dx.doi.org/10.1021/jp3100798 | J. Phys. Chem. A 2013, 117, 2605−2618

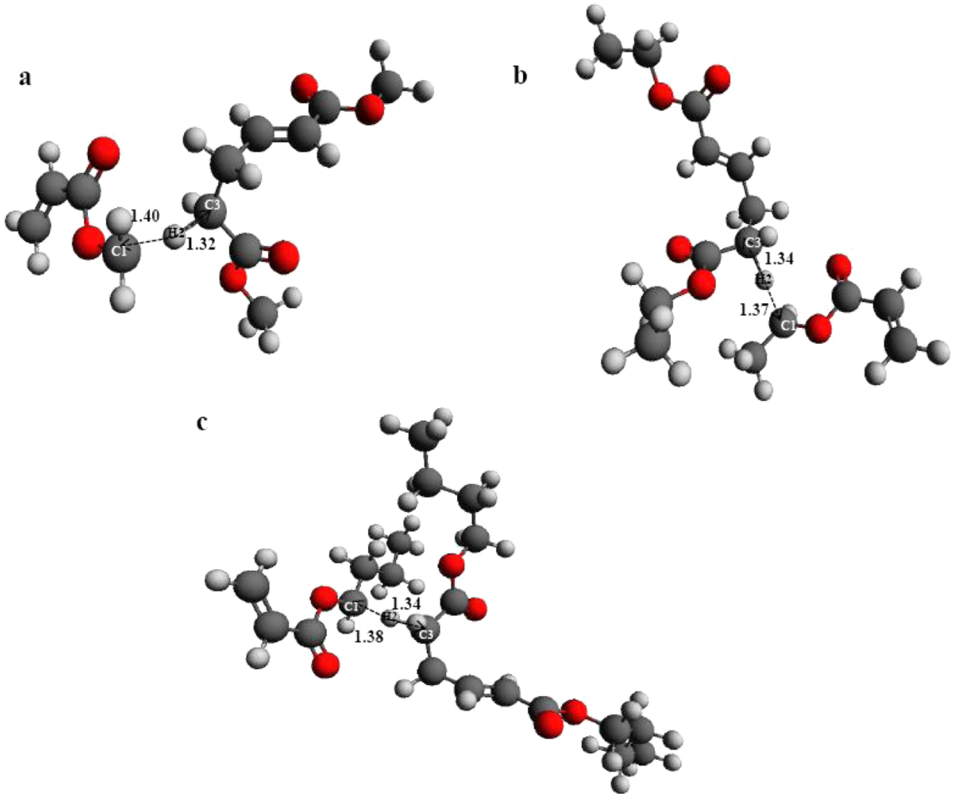

Figure 2. Transition state geometry of the three mechanisms: (a) MA-1, (b) EA-1, and (c) *n*-BA-1 (bond length in Å).

Scheme 2. Possible End-Chain Transfer to Monomer Reactions of EA (Et=Ethyl)

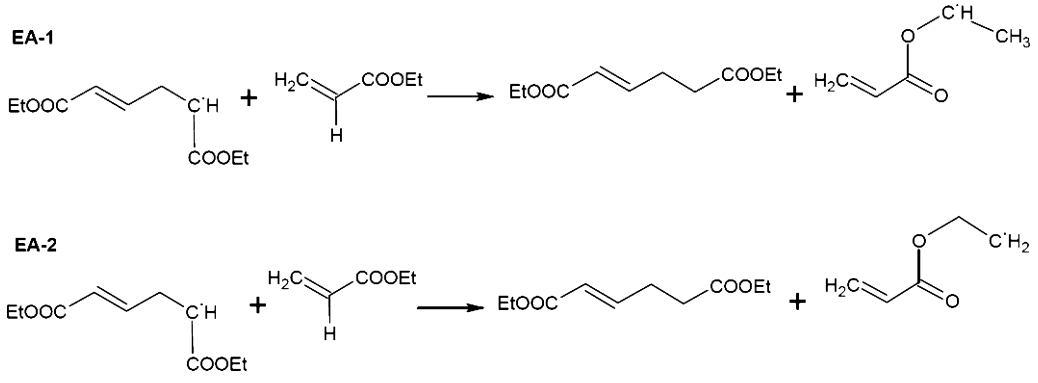

Table 3. Activation Energy (E_a), Enthalpy of Activation ($\Delta H^{\ddagger}$), and Gibb's Free Energy of Activation ($\Delta G^{\ddagger}$) in kJ mol^{-1}; Frequency Factor (A) and Rate Constant (k) in M^{-1} s^{-1} for the Two CTM Reactions of EA at 298 K.

	B3LYP 6-31G(d)	B3LYP 6-31G(d,p)	B3LYP 6-311G(d)	B3LYP 6-311G(d,p)	X3LYP 6-31G(d,p)	X3LYP 6-311G(d)	X3LYP 6-311G(d,p)	M06-2X 6-31G(d,p)	M06-2X 6-311G(d)	M06-2X 6-311G(d,p)
Hydrogen Abstraction via EA-1										
E_a	56	54	60	57	50	56	54	41	40	44
$\Delta H^{\ddagger}$	51	49	55	52	45	51	49	36	35	39
$\Delta G^{\ddagger}$	106	103	110	107	100	107	104	92	92	95
$\log_e A$	12.57	12.8	12.37	12.78	12.54	12.37	12.25	11.75	11.74	11.78
k	4.1×10^{-05}	1.4×10^{-04}	7.2×10^{-06}	3.2×10^{-05}	4.6×10^{-04}	3.1×10^{-05}	7.7×10^{-05}	9.9×10^{-03}	1.4×10^{-02}	3.1×10^{-03}
Hydrogen Abstraction via EA-2										
E_a	74	72	79	78	67	73	73	45	55	51
$\Delta H^{\ddagger}$	69	67	74	73	62	68	68	40	50	46
$\Delta G^{\ddagger}$	125	122	129	119	119	121	115	108	110	106
$\log_e A$	12.23	12.26	12.35	16.19	11.44	13.29	15.86	7.27	10.47	10.36
k	2.1×10^{-08}	6×10^{-08}	4×10^{-09}	2.4×10^{-07}	1.9×10^{-07}	8.5×10^{-08}	1.3×10^{-06}	2.2×10^{-05}	7.5×10^{-06}	3.5×10^{-05}

dx.doi.org/10.1021/jp3100798 | J. Phys. Chem. A 2013, 117, 2605−2618

Scheme 3. Possible End-Chain Transfer to Monomer Reactions of *n*-BA (Bu=Butyl)

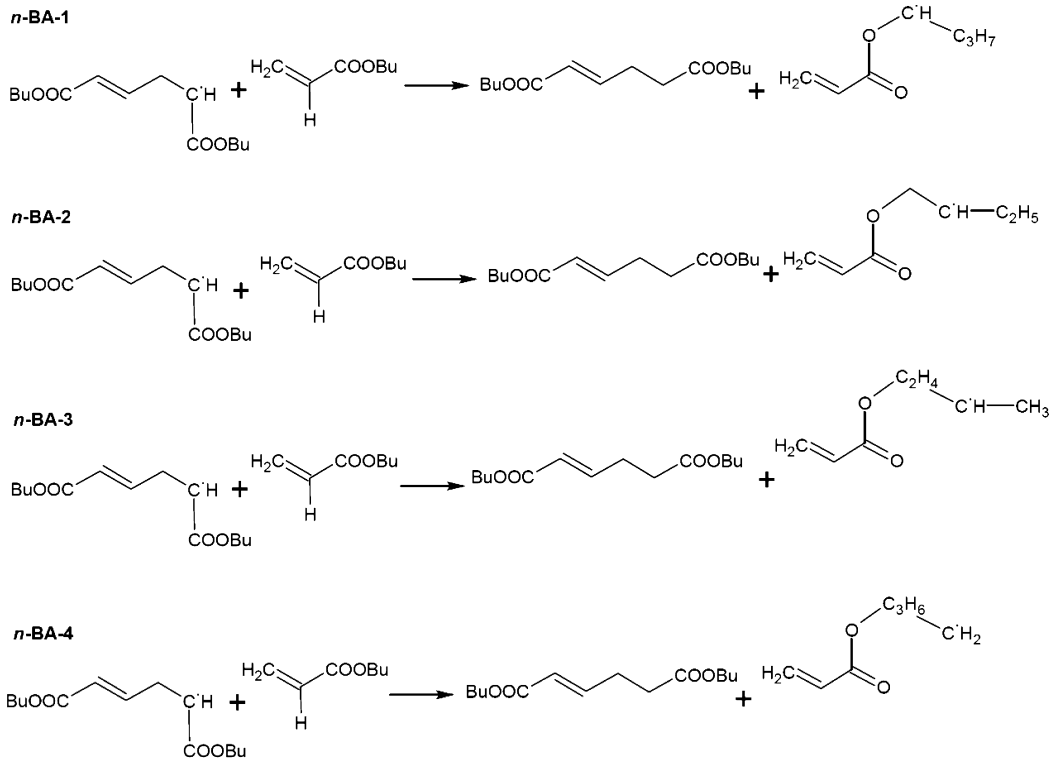

Table 4. Activation Energy (E_a), Enthalpy of Activation ($\Delta H^{\ddagger}$), and Gibb's Free Energy of Activation ($\Delta G^{\ddagger}$) in kJ mol^{-1}; Frequency Factor (A) and Rate Constant (k) in M^{-1} s^{-1} for the Four CTM Reactions of *n*-BA at 298 K

	B3LYP 6-31G(d)	B3LYP 6-31G(d,p)	B3LYP 6-311G(d)	B3LYP 6-311G(d,p)	X3LYP 6-31G(d,p)	X3LYP 6-311G(d)	X3LYP 6-311G(d,p)	M06-2X 6-31G(d,p)	M06-2X 6-311G(d)	M06-2X 6-311G(d,p)
					Hydrogen Abstraction via *n*-BA-1					
E_a	51	47	55	53	42	51	49	31	36	43
$\Delta H^{\ddagger}$	46	42	50	48	37	46	44	26	31	38
$\Delta G^{\ddagger}$	106	111	107	110	105	108	106	83	89	96
$\log_e A$	10.48	6.73	11.68	9.62	7.25	9.49	9.56	11.9	11.09	11.37
k	4.1×10^{-05}	5.7×10^{-06}	3.2×10^{-05}	8.3×10^{-06}	6.6×10^{-05}	1.5×10^{-05}	4.2×10^{-05}	0.5	0.04	2.3×10^{-03}
					Hydrogen Abstraction via *n*-BA-2					
E_a	66	64	68	70	52	60	60	26	33	30
$\Delta H^{\ddagger}$	61	59	63	65	47	55	55	21	28	25
$\Delta G^{\ddagger}$	110	107	120	109	115	125	116	89	87	92
$\log_e A$	14.86	14.98	11.73	17.05	7.01	6.43	10.08	7.57	10.88	7.65
k	8.4×10^{-06}	2.3×10^{-05}	1.7×10^{-07}	1.2×10^{-05}	9×10^{-07}	1.9×10^{-08}	8.2×10^{-07}	4.5×10^{-02}	7.9×10^{-02}	9.6×10^{-03}
					Hydrogen Abstraction via *n*-BA-3					
E_a	67	66	66	66	59	65	63	40	45	45
$\Delta H^{\ddagger}$	63	61	61	61	54	60	58	34	40	40
$\Delta G^{\ddagger}$	114	113	111	104	113	115	122	100	98	100
$\log_e A$	14.22	13.70	14.41	17.4	10.6	12.46	8.62	8.26	11.2	10.64
k	1.9×10^{-06}	2.7×10^{-06}	6×10^{-06}	9.4×10^{-05}	2.1×10^{-06}	1.1×10^{-06}	5.6×10^{-08}	5.2×10^{-04}	9.8×10^{-04}	5.2×10^{-04}
					Hydrogen Abstraction via *n*-BA-4					
E_a	70	68	72	72	63	70	68	53	53	55
$\Delta H^{\ddagger}$	65	62	67	67	58	65	63	48	48	50
$\Delta G^{\ddagger}$	130	129	131	127	125	126	125	110	117	111
$\log_e A$	8.01	7.8	8.58	10.28	7.52	10.21	9.49	9.74	6.51	9.96
k	2×10^{-09}	3.9×10^{-09}	1.4×10^{-09}	7.7×10^{-09}	1.7×10^{-08}	1.4×10^{-08}	1.6×10^{-08}	9.1×10^{-06}	4×10^{-07}	4.8×10^{-06}
exptl[19]			E_a = 31 kJ mol^{-1}				k = 0.6 M^{-1} s^{-1}			

0.960, 0.961, 0.966, and 0.967 are used for the B3LYP functional with the 6-31G(d), 6-31G(d,p), 6-311G(d), and 6-311G(d,p) basis sets, respectively. These factors were obtained from the National Institute of Standards and Technology (NIST) scientific and technical database.[82]

3. RESULTS AND DISCUSSION

3.1. Chain Transfer to Monomer Mechanisms for $M_2^{\bullet}$.

3.1.1. Methyl Acrylate. As shown in Scheme 1, we have studied four CTM mechanisms of methyl acrylate chains initiated by

dx.doi.org/10.1021/jp3100798 | J. Phys. Chem. A 2013, 117, 2605−2618

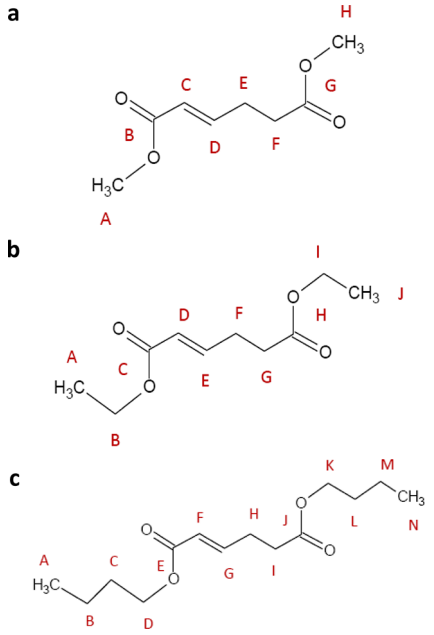

Figure 3. Dead polymer chains generated via the MA-1, EA-1, and *n*-BA-1 mechanisms: (a) MA-1, (b) EA-1, and (c) *n*-BA-1.

$M_2^\bullet$ radical. The mechanisms are abstraction of a methyl hydrogen atom from the monomer by a live chain (MA-1), abstraction of a vinylic hydrogen atom from the monomer (MA-2), abstraction of a methine hydrogen atom from the monomer (MA-3), and transfer of a hydrogen atom from a live polymer chain to the monomer (MA-4). These mechanisms are studied by choosing *r*(H2−C3) and *r*(C1−H2) as reaction coordinates. The potential energy surface is sampled by varying C−H bond lengths between 1.19 and 1.59 Å.

The activation energies, activation enthalpies, frequency factors, free energies of activation, and rate constants of the four mechanisms are given in Table 1. It was determined using different levels of theory that MA-1 is the most kinetically favorable mechanism, and MA-2, MA-3, and MA-4 mechanisms have higher activation energies. This agrees with the finding that the bond-dissociation energy of a methyl hydrogen is lower than that of a methine hydrogen and a vinylic hydrogen, as given in Table 2. The difference in the bond-dissociation energies can be attributed to the lower stability of the vinyl radical.[83,84] In this study, bond-dissociation energy is defined as the energy difference between a monomer molecule and bond cleavage products (hydrogen radical and monomer mono-radical):[85]

$$\text{bond dissociation energy} = E_{(\text{bond cleavage products})} - E_{(\text{monomer})} \quad (5)$$

It represents the energy required to break a carbon−hydrogen bond of a molecule; it is a measure of the strength of a C−H bond.

Mulliken charge analysis also reveals that the methyl carbon atom (−0.117) is more positive than vinylic carbon atoms (−0.247 and −0.126), and therefore, more likely to release a hydrogen atom. Figure 2a shows the transition-state geometry for the MA-1 mechanism, which has H2−C3 and C1−H2 bond lengths of 1.32 and 1.40 Å, respectively. We found that the computed thermodynamic quantities (activation energy and rate constants) are not sensitive to the size of basis sets (6-31G(d), 6-31G(d,p), and 6-311G(d)), but vary significantly depending on the type of density functionals. For a given density functional, the difference in calculated energy barrier using different basis sets (6-31G(d), 6-31G(d,p), and 6-311G(d)) is generally below 6 kJ mol^{-1}. Changing the type of functional, however, can result in a ∼15 kJ mol^{-1} difference in barrier height and 2 orders of magnitude difference in rate constants. The functional has more impact on the predicted barriers than the basis set for studying chain transfer reactions of methyl acrylate.

3.1.2. Ethyl Acrylate. For EA, two CTM mechanisms of ethyl acrylate chains initiated by $M_2^\bullet$ radicals, as shown in Scheme 2, are considered. These are the abstraction of a methylene hydrogen atom (EA-1) and abstraction of a methyl hydrogen atom (EA-2). Abstraction of methine and vinylic hydrogens from EA are not studied, as our studies on MA already showed that these reactions have higher energy barriers. Abstraction of hydrogen from EA-1 and EA-2 is investigated by constraining C1−H2 and H2−C3 bond lengths between 1.19 and 1.59 Å. The transition-state structure for the EA-1 mechanism has H2−C3 and C1−H2 bond lengths of 1.34 and 1.37 Å, respectively (Figure 2b). The activation energies and rate constants for these mechanisms are given in Table 3. The barrier of the EA-1 mechanism was found to be lower than that of EA-2 mechanism. It can be seen from the Mulliken charges of the ethyl acrylate carbon atoms (methylene carbon atom = 0.01, methyl carbon atom = −0.383, and vinylic carbon atom = −0.12 and −0.26) that the methylene carbon is more electrophilic, indicating its higher tendency to donate a proton. This also agrees with the finding that the bond-dissociation energy of the side-chain methylene group in EA-1 was lower than that of the methine group (Table 2). Therefore, the occurrence of the EA-1 chain transfer mechanism in thermal polymerization of EA is highly probable.

3.1.3. n-Butyl Acrylate. We studied four CTM mechanisms for *n*-BA chains initiated by $M_2^\bullet$ radical as shown in Scheme 3. These are abstraction of a hydrogen atom from three different methylene groups (*n*-BA-1, *n*-BA-2, and *n*-BA-3) and abstraction of a methyl hydrogen atom (*n*-BA-4). These mechanisms are investigated by constraining the C1−H2 and H2−C3 bond lengths between 1.19 and 1.59 Å. The transition-state structure for the *n*-BA-1 reaction is shown in Figure 2c. Its geometry has H2−C3 and C1−H2 bond lengths of 1.34 and 1.38 Å, respectively. Table 4 lists the activation energies and rate constants for the reactions. We determined that the rate constant of *n*-BA-1 is significantly higher than that of *n*-BA-2, *n*-BA-3, and *n*-BA-4 with different levels of theory. It was identified that the abstraction of a hydrogen atom from a methylene group adjacent to methyl group in the butyl side chain has higher activation energy than that of the other methylene hydrogen atoms (Table 4). Mulliken charge analysis reveals that the methylene group carbon next to the ester oxygen of the end-substituent butyl group (0.022) is more electrophilic in comparison to the other methylene carbon atoms (−0.269 and −0.18) and methyl carbon atom (−0.37). Therefore, the hydrogen atom is more likely released from that methylene group. The bond-dissociation energy given in Table 2 also indicates that the C−H bond in a methylene group is much weaker than that in a methyl group. We found that the calculated activation energy and rate constant of hydrogen abstraction from the methylene group adjacent to the ester oxygen of the butyl side chain using M06-2X/6-31G(d,p) was quite similar to experimental values.[19] The calculated activation

dx.doi.org/10.1021/jp3100798 | J. Phys. Chem. A 2013, 117, 2605−2618

Table 5. Assignment of ^{13}C NMR Spectra for MA, EA, and *n*-BA (Chemical Shifts Are Relative to TMS with Absolute Isotropic Shielding of 187 ppm for the ^{13}C)

description	details	calcd peaks	exptl peaks[14,71]
carbonyl C			
	COOX next to the terminal saturation	177.6−179.2	
		X = CH_3	
		177.2−179	172.7−172.9
		X = CH_2CH_3	
		177.1−179	
		X = $CH_2CH_2CH_2CH_3$	
	COOX next to the terminal unsaturation	171.1−173	
		X = CH_3	
		170−172.5	166.4−166.7
		X = CH_2CH_3	
		170.6−172.5	
		X = CH2CH2CH2CH3	
CH in the main chain			
	methine group in the main chain, CH next to the COOX	130.8−131.6	
		X = CH_3	
		130.8−131.5	125.4−126
		X = CH_2CH_3	
		130.8−131.4	
		X = $CH_2CH_2CH_2CH_3$	
	methine group in the main chain of MA, CH	155.2−156.1	
	methine group in the main chain of EA, CH	155.2−156.2	137.7−137.9
	methine group in the main chain of BA, CH	155.4−156.3	
CH_2 on the side chain, close to terminal saturation			
	CH_2 on the ethyl side chain	66.3−67	60.4−60.9
	CH_2 on the butyl side chain, next to the ester oxygen	70.5−71.6	
	CH_2 in the middle of the butyl side chain	36.1−36.4	30.5
	CH_2 on the butyl side chain, prior to methyl group	24.3−24.8	30.5
CH_2 on the side chain, close to terminal unsaturation			
	CH_2 on the ethyl side chain	65.6−66.4	60.4−60.9
	CH_2 on the butyl side chain, next to the ester oxygen	70.4−71	
	CH_2 in the middle of the butyl side chain	36.3−36.7	30.5
	CH_2 on the butyl side chain, prior to methyl group	24.5−25	30.5
CH_2 in the main chain			
	CH_2 next to the COOX	35.3−36.1	
		X = CH_3	
		35.5−36.7	33.2−37
		X = CH2CH_3	
		35.9−36.9	33.7−37.4
		X = $CH_2CH_2CH_2CH_3$	
	CH_2 in the main chain of MA, close to the double bond	31.5−32.6	
	CH_2 in the main chain of EA, close to the double bond	31.6−32.8	28−29.6
	CH_2 in the main chain of BA, close to the double bond	32.3−33.5	33.7−37.4
CH_3			
	C in O−CH_3, close to terminal saturation	55−55.7	
	C in O−CH_3, close to terminal unsaturation	54.6−55.2	
	C in the end group CH_3, on the ethyl side chain, close to terminal saturation	15.8−16.3	14.20
	C in the end group CH_3, on the ethyl side chain, close to terminal unsaturation	16−16.5	14.20
	C in the end group CH_3, on the butyl side chain, close to terminal saturation	16.9−17.4	
	C in the end group CH_3, on the butyl side chain, close to terminal unsaturation	17−17.5	

energy and the rate constant are 31 kJ mol^{-1} and 0.5 $L{\cdot}mol^{-1}{\cdot}s^{-1}$, and the experimental values are 31 kJ mol^{-1} and 0.6 $L{\cdot}mol^{-1}{\cdot}s^{-1}$.[19,22] We observe no significant difference in the activation energies and rate constants for abstracting a hydrogen atom from the three methylene groups of *n*-BA, while a previous study[19] had reported that the two middle methylene groups of the side chain have the lowest barriers for releasing a hydrogen atom. The lowest energy mechanisms in

dx.doi.org/10.1021/jp3100798 | J. Phys. Chem. A 2013, 117, 2605−2618

Scheme 4. Most Probable Mechanisms for CTM Reactions Involving a Two-Monomer-Unit Live Chain Initiated by $M_1^{\bullet}$

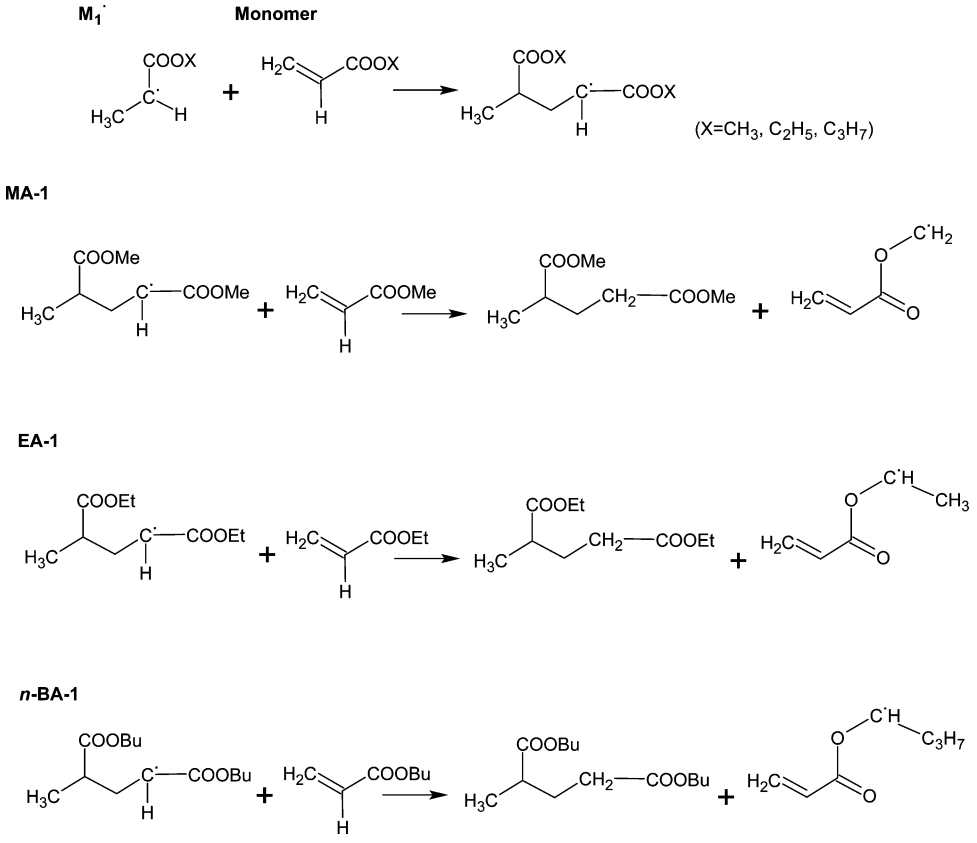

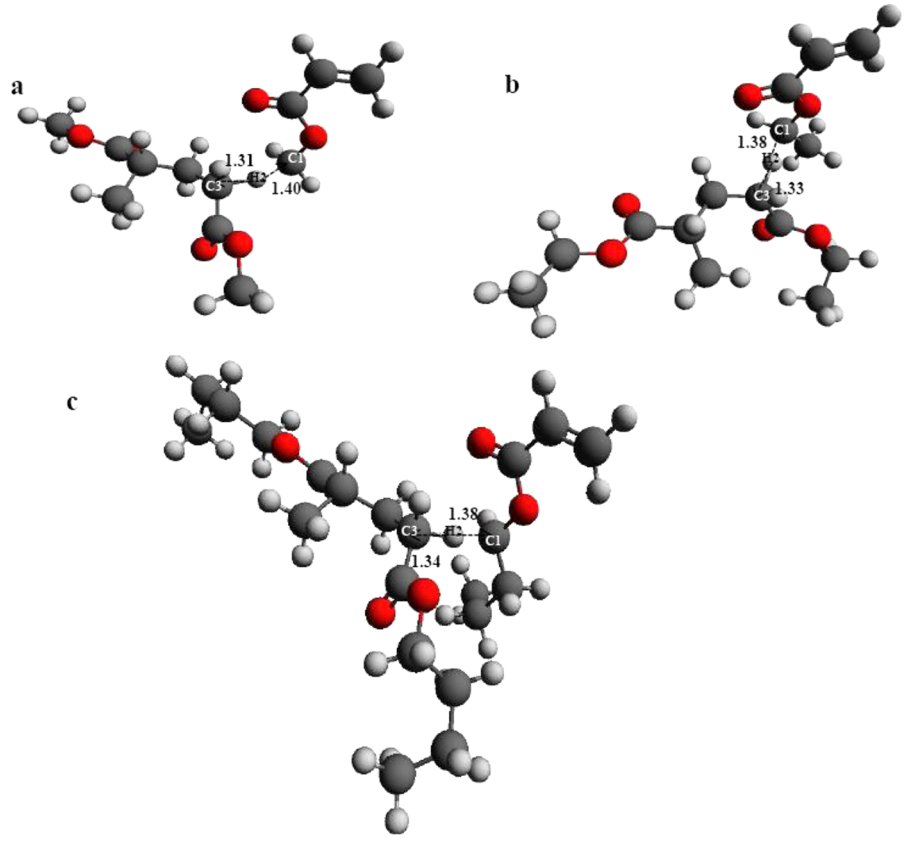

Figure 4. Transition state geometries of (a) MA-1, (b) EA-1, and (c) *n*-BA-1 for mechanisms involving a two-monomer-unit live chain initiated by $M_1^{\bullet}$ (bond length in Å).

dx.doi.org/10.1021/jp3100798 | J. Phys. Chem. A 2013, 117, 2605−2618

Table 6. Activation Energy (E_a), Enthalpy of Activation ($\Delta H^{\ddagger}$), and Gibb's Free Energy of Activation ($\Delta G^{\ddagger}$) in kJ mol^{-1}; Frequency Factor (A) and Rate Constant (k) in M^{-1} s^{-1} of the MA-1, EA-1, and *n*-BA-1 Reactions Involving Two-Monomer-Unit Live Chains Initiated by $M_1^{\bullet}$ at 298 K

	B3LYP 6-31G(d)	B3LYP 6-31G(d,p)	B3LYP 6-311G(d)	B3LYP 6-311G(d,p)	X3LYP 6-31G(d,p)	X3LYP 6-311G(d)	X3LYP 6-311G(d,p)	M06-2X 6-31G(d,p)	M06-2X 6-311G(d)	M06-2X 6-311G(d,p)
					MA-1					
E_a	78	76	81	78	68	75	73	63	67	65
$\Delta H^{\ddagger}$	73	71	76	73	63	71	68	58	62	60
$\Delta G^{\ddagger}$	120	117	124	120	124	126	123	115	119	118
$\log_e A$	15.58	15.9	15.28	15.65	9.89	12.27	12.43	11.63	11.5	11.35
k	1.2×10^{-07}	4.3×10^{-07}	2.7×10^{-08}	1.3×10^{-07}	2.7×10^{-08}	1.3×10^{-08}	4.9×10^{-08}	1.3×10^{-06}	1.9×10^{-07}	3.8×10^{-07}
					EA-1					
E_a	63	60	69	69	62	65	65	48	49	52
$\Delta H^{\ddagger}$	58	56	64	64	57	60	60	43	44	48
$\Delta G^{\ddagger}$	115	113	114	107	97	110	101	101	91	94
$\log_e A$	11.68	11.66	14.30	17.43	18.47	14.56	17.96	10.97	15.55	15.76
k	1.1×10^{-06}	2.9×10^{-06}	1.5×10^{-06}	3.3×10^{-05}	1.7×10^{-03}	8.6×10^{-06}	2.6×10^{-04}	2.7×10^{-04}	1.8×10^{-02}	4.4×10^{-03}
					n-BA-1					
E_a	67	65	71	71	64	68	66	57	59	59
$\Delta H^{\ddagger}$	62	60	66	66	59	63	61	52	54	54
$\Delta G^{\ddagger}$	111	109	112	103	100	110	108	90	99	103
$\log_e A$	14.75	14.9	15.97	19.83	18.28	15.56	15.41	19.46	16.34	14.9
k	4.5×10^{-06}	1.1×10^{-05}	3.1×10^{-06}	1.3×10^{-04}	4.9×10^{-04}	7.3×10^{-06}	1.5×10^{-05}	2.9×10^{-02}	5.7×10^{-04}	1.3×10^{-04}

Scheme 5. Most Probable Mechanisms for CTM Reactions Involving a Three-Monomer-Unit Live Chain Initiated by $M_2^{\bullet}$

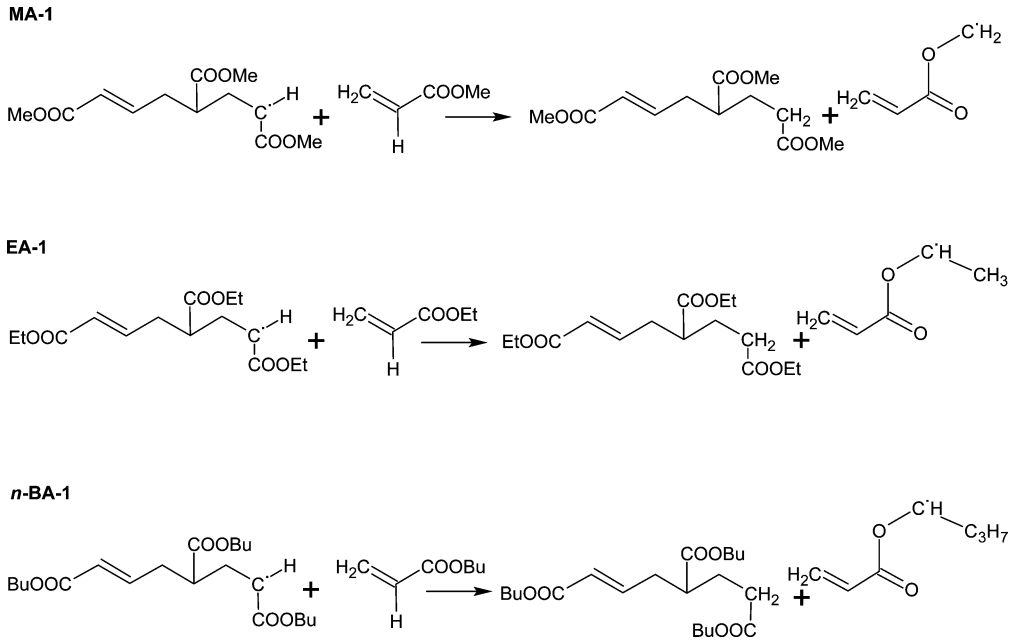

MA, EA, and *n*-BA were compared, and it was identified that the activation energy of MA-1 (Table 1) is higher than that of EA-1 (Table 3) or *n*-BA-1 (Table 4). As reported in Tables 1, 3, and 4, the activation energy for the most favorable CTM mechanism in MA (MA-1) is much higher (~20 kJ/mol) than those for the most favorable ones in EA (EA-1) and *n*-BA (*n*-BA-1, *n*-BA-2, and *n*-BA-3). More precisely, the bond dissociation energy of a methyl hydrogen atom in MA is higher than that of methylene hydrogen atoms in EA and *n*-BA. This indicated that the type of the hydrogen atom influences the height of the barrier.

We compute the ^{13}C NMR chemical shifts of the dead polymer chains formed by the most probable CTM mechanisms (MA-1, EA-1, and *n*-BA-1) using ORCA.[74] Figure 3 shows these polymer chains. We have applied different methods (B3LYP and X3LYP) and basis sets (6-31G(d), 6-31G(d,p), 6-311G(d), and 6-311G(d,p)) for calculating the chemical shifts. All the functionals give similar results for the chemical shifts. The calculated NMR chemical shifts for the dead polymer chains generated via the MA-1, EA-1, and *n*-BA-1 mechanisms, given in Table 5, are comparable with experimental values reported in spontaneous polymerization of *n*-BA.[14,73]

This agreement suggests that the mechanisms found to be kinetically favorable are most likely occurring in thermal polymerization of alkyl acrylates. No experimental NMR chemical shift in spontaneous polymerization was found to be similar to the calculated results for the chemical shifts of the product generated from the MA-4 mechanism. On the basis of these comparisons, one can conclude that the MA-4

dx.doi.org/10.1021/jp3100798 | J. Phys. Chem. A 2013, 117, 2605−2618

Table 7. Activation Energy (E_a), Enthalpy of Activation ($\Delta H^{\ddagger}$), and Gibb's Free Energy of Activation ($\Delta G^{\ddagger}$) in kJ mol^{-1}; Frequency Factor (A) and Rate Constant (k) in M^{-1} s^{-1} of the MA-1, EA-1, and *n*-BA-1 Reactions Involving Three-Monomer-Unit Live Chains Initiated by $M_2^{\bullet}$ at 298 K Calculated Using B3LYP/6-31G(d) and M06-2X/6-31G(d,p)

	E_a	$\Delta H^{\ddagger}$	$\Delta G^{\ddagger}$	$\log_e A$	k
			MA-1		
B3LYP	69	64	120	12.07	1.2×10^{-7}
M06-2X	55	50	102	13.63	2×10^{-4}
			EA-1		
B3LYP	55	50	108	11.2	1.5×10^{-5}
M06-2X	35	30	93	9.53	9.2×10^{-3}
			n-BA-1		
B3LYP	52	48	125	3.5	2.1×10^{-8}
M06-2X	54	49	102	13.22	1.7×10^{-4}

mechanism does not seem to be the most favorable one for CTM reactions. The energy differences of the optimized reactants and products for the CTM mechanisms in MA, EA, and *n*-BA are reported in the Supporting Information.

3.2. Chain Transfer to Monomer Mechanisms for $M_1^{\bullet}$. As shown in Scheme 4, the chain transfer reactions, MA-1, EA-1, and *n*-BA-1, of a 2-monomer-unit live polymer chain initiated via $M_1^{\bullet}$ are investigated using B3LYP, X3LYP, and M06-2X functionals. The calculated transition states have C1−H2 and H2−C3 bond lengths of 1.31 and 1.40 Å in MA, 1.33 and 1.38 Å in EA, and 1.34 and 1.38 Å in *n*-BA. The transition state structures for these mechanisms are shown in Figure 4, and activation energies and rate constants are given in Table 6. Comparing these results with those calculated in the previous section for $M_2^{\bullet}$ initiated chains shows little difference in activation energy and rate constants, which indicates that the type of initiating radical of the live polymer chain has little effect on the rate of the CTM reactions.

3.3. Effect of Live Polymer Chain Length. To understand the effect of polymer chain length on the kinetics of CTM, we investigated MA-1, EA-1, and *n*-BA-1 mechanisms with a 3-monomer-unit live chain initiated via $M_2^{\bullet}$ (Scheme 5). We constrained the C1−H2 and H2−C3 bond lengths between 1.19 and 1.59 Å in the three mechanisms. We found the bond lengths of H2−C3 and C1−H2 of the transition state to be

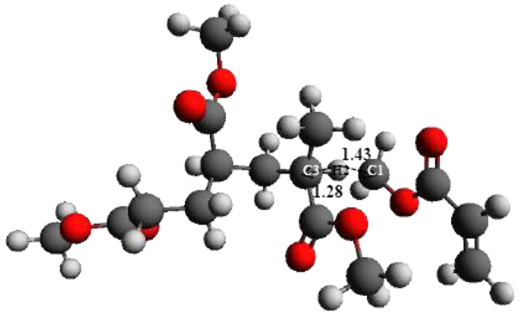

Figure 5. Transition state geometry of MA-1 reaction involving the live chain $Q_3^{\bullet}$ (bond length in Å).

Table 8. Activation Energy (E_a) and Enthalpy of Activation ($\Delta H^{\ddagger}$) in kJ mol^{-1}; Frequency Factor (A) and Rate Constant (k) in M^{-1} s^{-1} of the MA-1 Reaction Involving Three-Monomer-Unit Live Chains Initiated by $M_1^{\bullet}$ at 298 K Calculated Using M06-2X/6-31G(d,p) (the bonds are shown in Figure 5)

C1−H2 (Å)	C3−H2 (Å)	E_a	$\Delta H^{\ddagger}$	$\log_e A$	k
		Secondary Live Chain			
1.40	1.32	55	50	12.89	8.3×10^{-5}
		Tertiary Live Chain			
1.43	1.28	67	62	9.93	3.5×10^{-8}

1.31 and 1.4 Å in MA, 1.33 and 1.38 Å in EA, and 1.34 and 1.38 Å in *n*-BA. It was observed that the transition-state geometries of 3-monomer-unit live chains are similar to those of 2-monomer-unit live chains discussed in section 3.1. It can be concluded that the live polymer chain length does not significantly affect the geometry of the reaction center. As given in Table 7, the calculated activation energies of the CTM reactions using B3LYP/6-31G(d) vary very little with the length of the polymer chain. However, M06-2X/6-31G(d,p) did show increase in the energy barrier for *n*-BA-1 with increasing chain length. This is likely due to the long-range exchange interactions in the hybrid meta-functional M06-2X.

3.4. Effect of Radical Location in a Live Chain. Previous studies[1,2,14] have shown that inter- and intramolecular chain transfer reactions occur at high rates at high temperatures (>100 °C), which can lead to the formation of tertiary radicals[14] and that both the secondary and tertiary radicals are

Scheme 6. CTM Reaction Involving the Live Chain $Q_3^{\bullet}$ and $P_3^{\bullet}$ Initiated by $M_1^{\bullet}$ (Me=Methyl)

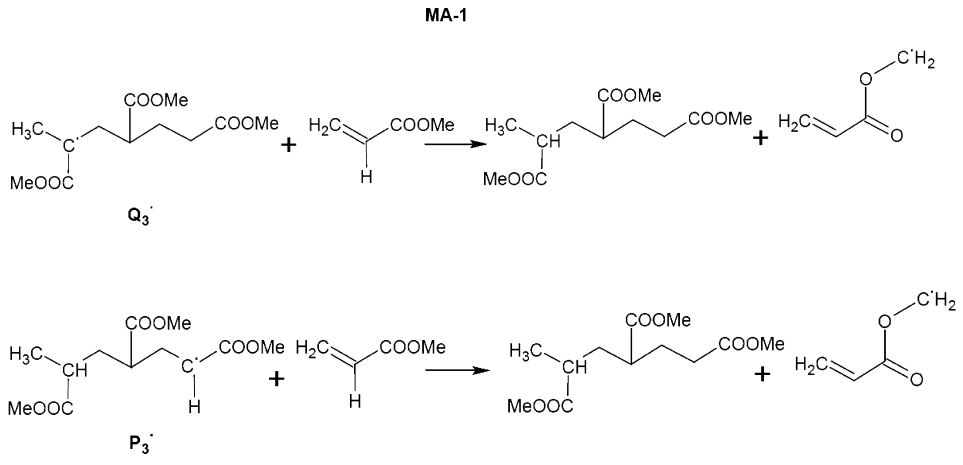

dx.doi.org/10.1021/jp3100798 | J. Phys. Chem. A 2013, 117, 2605−2618

capable of initiating polymer chains. We also studied the CTM reactions of an $M_1^\bullet$-initiated three-monomer-unit live chain with a secondary radical, denoted by $P_3^\bullet$, and an $M_1^\bullet$-initiated three-monomer-unit live chain with a tertiary radical, denoted by $Q_3^\bullet$, as shown in Scheme 6. The H2−C3 and C1−H2 bond lengths of the transition state of the MA-1 mechanism involving the $Q_3^\bullet$ live chain was found to be 1.28 and 1.43 Å, respectively (Figure 5). The calculated energy barriers and rate constants of these two mechanisms are given in Table 8. The activation energy of hydrogen abstraction by a tertiary radical is higher than that of hydrogen abstraction by a secondary radical. This suggests that the tertiary radical center probably prefers to react with a monomer and form chain branches or undergo β-scission reaction, rather than abstracting hydrogen atoms. This agrees with previous reports,[13,14] where NMR and mass spectrometry have shown the formation of chain branches from tertiary radicals.

4. CONCLUDING REMARKS

The mechanisms for chain transfer to monomer in self-initiated high-temperature polymerization of three alkyl acrylates were studied using different levels of theory. Abstraction of a methylene group hydrogen by a live polymer chain in EA and *n*-BA and a methyl group hydrogen in MA were found to be the favorable mechanisms for chain transfer to monomer reaction. The kinetic parameters calculated using M06-2X/6-31G(d,p) are closest to those estimated from polymer sample measurement. The C−H bond lengths of transition state structures for CTM reactions in MA, EA, and *n*-BA were found to be insensitive to the choice of functionals. NMR spectra of various reacting species in CTM reactions in MA, EA, and *n*-BA were predicted. The NMR chemical shifts of dead polymer chains from MA-1, EA-1, and *n*-BA-1 are comparable to those from polymer sample analyses, which confirms that the products of the chain transfer reactions proposed in this study are formed in polymerization of MA, EA, and *n*-BA. It was found that the polymer chain length had little effect on the activation energies and rate constants of the mechanisms of CTM reaction when applying B3LYP/6-31G(d) functional. However, M06-2X/6-31G(d,p) showed differences between the kinetic parameters of CTM reactions involving live chains with two and three monomer units. MA, EA, and *n*-BA live chains initiated by $M_2^\bullet$ and those initiated by $M_1^\bullet$ showed similar hydrogen abstraction abilities, which indicates the lesser influence of self-initiating species on CTM reaction. Hydrogen abstraction by a tertiary radical has a much larger energy barrier than abstraction by a secondary radical.

■ ASSOCIATED CONTENT

Supporting Information

Transition state geometries of the MA-1, EA-1, and *n*-BA-1 mechanisms involving a three-monomer-unit live chain initiated by $M_2^\bullet$, ^{13}C NMR spectra of the dead polymer chains generated via the MA-1, EA-1, and *n*-BA-1 mechanisms, and energy differences of the optimized reactants and products for the CTM mechanisms in MA, EA, and *n*-BA homopolymerization. This material is available free of charge via the Internet at http://pubs.acs.org.

■ AUTHOR INFORMATION

Corresponding Author

*Phone: (215) 895-1710. E-mail: ms1@drexel.edu.

Notes

The authors declare no competing financial interest.

■ ACKNOWLEDGMENTS

This material is based upon work partially supported by the National Science Foundation under Grants No. CBET-0932882, CBET-1160169 and CBET-1159736. Any opinions, findings, and conclusions or recommendations expressed in this material are those of the authors and do not necessarily reflect the views of the National Science Foundation. Acknowledgment is also made to the Donors of the American Chemical Society Petroleum Research Fund for partial support of this research. S.L. was supported by National Science Foundation Grant CBET-1159736. A.M.R. acknowledges the Air Force Office of Scientific Research, through grant FA9550-10-1-0248. Computational support was provided by the High-Performance Computing Modernization Office of the U.S. Department of Defense.

■ REFERENCES

(1) Grady, M. C.; Simonsick, W. J.; Hutchinson, R. A. Studies of Higher Temperature Polymerization of *n*-Butyl Methacrylate and *n*-Butyl Acrylate. *Macromol. Symp.* **2002**, *182*, 149−168.

(2) Rantow, F. S.; Soroush, M.; Grady, M.; Kalfas, G. Spontaneous Polymerization and Chain Microstructure Evolution in High Temperature Solution Polymerization of *n*-Butyl Acrylate. *Polymer* **2006**, *47*, 1423−1435.

(3) Barth, J.; Buback, M.; Russell, G. T.; Smolne, S. Chain-Length-Dependent Termination in Radical Polymerization of Acrylates. *Mol. Chem. Phys.* **2011**, *212*, 1366−1378.

(4) O'Leary, K.; Paul, D. R. Copolymers of Poly (*n*-Alkyl Acrylate): Synthesis, Characterization, and Monomer Reactivity Ratios. *Polymer* **2004**, *45*, 6575−6585.

(5) Mueller, P. A.; Richards, J. R.; Comgalidis, J. P. Polymerization Reactor Modeling in Industry. *Macromol. React. Eng.* **2011**, *5*, 261−277.

(6) *Superintendent of Documents, Title 1*; US Government Printing Office: Washington, DC, 1990; p 1.

(7) *Superintendent of Documents, Clean Air Act Amendments of 1990, Title 111*; US Government Printing Office: Washington, DC, 1990; p 236.

(8) Reisch, R. S. Paints & Coatings. *Chem. Eng. News* **1993**, *71* (42), 34.

(9) Chiefari, J.; Jeffery, J.; Mayadunne, R. T. A.; Moad, G.; Rizzardo, E.; Thang, S. H. Chain Transfer to Polymer: A Convenient Route to Macromonomers. *Macromolecules* **1999**, *32*, 7700−7702.

(10) Buback, M.; Klingbeil, S.; Sandmann, J.; Sderra, M. B.; Vogele, H. P.; Wackerbarth, H.; Wittkowski, L. Pressure and Temperature Dependence of the Decomposition Rate of *tert*-Butyl Peroxyacetate and of *tert*-Butyl Peroxypivalate. *Z. Phys. Chem.* **1999**, *210*, 199−221.

(11) Srinivasan, S.; Lee, M. W.; Grady, M. C.; Soroush, M.; Rappe, A. M. Self-Initiation Mechanism in Spontaneous Thermal Polymerization of Ethyl and *n*-Butyl Acrylate: A Theoretical Study. *J. Phys. Chem. A* **2010**, *114*, 7975−7983.

(12) Srinivasan, S.; Lee, M. W.; Grady, M. C.; Soroush, M.; Rappe, A. M. Computational Study of the Self-Initiation Mechanism in Thermal Polymerization of Methyl Acrylate. *J. Phys. Chem. A* **2009**, *113*, 10787−10794.

(13) Nikitin, A. N.; Hutchinson, R. A.; Wang, W.; Kalfas, G. A.; Richards, J. R.; Bruni, C. Effect of Intramolecular Transfer to Polymer on Stationary Free-Radical Polymerization of Alkyl Acrylates, 5: Consideration of Solution Polymerization up to High Temperatures. *Macromol. React. Eng.* **2010**, *4*, 691−706.

(14) Quan, C.; Soroush, M.; Grady, M. C.; Hansen, J. E.; Simonsick, W. J. High-Temperature Homopolymerization of Ethyl Acrylate and *n*-Butyl Acrylate: Polymer Characterization. *Macromolecules* **2005**, *38*, 7619−7628.

(15) Peck, A. N. F.; Hutchinson, R. A. Secondary Reactions in the High Temperature Free Radical Polymerization of Butyl Acrylate. *Macromolecules* **2004**, *37*, 5944−5951.
(16) Srinivasan, S.; Kalfas, G.; Petkovska, V. I.; Bruni, C.; Grady, M. C.; Soroush, M. Experimental Study of Spontaneous Thermal Homopolymerization of Methyl and *n*-Butyl Acrylate. *J. Appl. Polym. Sci.* **2010**, *118*, 1898−1909.
(17) Gilbert, R. G. *Emulsion Polymerization. A Mechanistic Approach*; Academic Press: London, 1995.
(18) Odian, G.; *Priciples of Polymerization*, 3rd ed.; Wiley-Interscience: New York, 1991.
(19) Sangster, D. F.; Feldthusen, J.; Strauch, J.; Fellows, C. M. Measurement of Transfer Coefficient to Monomer for *n*-Butyl Methacrylate by Molecular Weight Distributions from Emulsion Polymerization. *Macromol. Chem. Phys.* **2008**, *209*, 1612−1627.
(20) Kukulj, D.; Davis, T. P.; Gilbert, R. G. Chain Transfer to Monomer in the Free-Radical Polymerizations of Methyl Methacrylate, Styrene, and α-Methylstyrene. *Macromolecules* **1998**, *31*, 994−999.
(21) Berkel, K. Y.; Russell, G. T.; Gilbert, R. G. Molecular Weight Distributions and Chain-Stopping Events in the Free-Radical Polymerization of Methyl Methacrylate. *Macromolecules* **2005**, *38*, 3214−3224.
(22) Maeder, S.; Gilbert, R. G. Measurement of Transfer Constant for Butyl Acrylate Free-Radical Polymerization. *Macromolecules* **1998**, *31*, 4410−4418.
(23) Chiefari, J.; Chong, Y. K.; Ercole, F.; Krstina, J.; Jeffery, J.; Le, T. P. T.; Mayadunne, R. T. A.; Meijs, G. F.; Moad, C. L.; Moad, G.; Rizzardo, E.; Thang, S. H. Living Free-Radical Polymerization by Reversible Addition−Fragmentation Chain Transfer: The RAFT Process. *Macromolecules* **1998**, *31*, 5559−5562.
(24) Le, T. P.; Moad, G.; Rizzardo, E.; Thang, S. H. Patent WO 9,801,478.
(25) Mayadunne, R. T. A.; Rizzardo, E.; Chiefari, J.; Chong, Y. K.; Moad, G.; Thang, S. H. Living Radical Polymerization with Reversible Addition−Fragmentation Chain Transfer (RAFT Polymerization) Using Dithiocarbamates as Chain Transfer Agents. *Macromolecules* **1999**, *32*, 6977−6980.
(26) Donovan, M. S.; Lowe, A. B.; Sumerlin, B. S.; McCormick, C. L. Raft Polymerization of *N*,*N*-Dimethylacrylamide Utilizing Novel Chain Transfer Agents Tailored for High Reinitiation Efficiency and Structural Control. *Macromolecules* **2002**, *35*, 4123−4132.
(27) Barner-Kowollik, C.; Davis, T. P.; Heuts, J. P.; Stenzel, M. H.; Vana, P.; Whittaker, M. RAFTing Down Under: Tales of Missing Radicals, Fancy Architectures and Mysterious Holes. *J. Polym. Sci., Part A: Polym. Chem.* **2003**, *41*, 365.
(28) Hawker, C. J.; Bosman, A. W.; Harth, E. New Polymer Synthesis by Nitroxide Mediated Living Radical Polymerizations. *Chem. Rev.* **2001**, *101*, 3661−3688.
(29) Matyjaszewski, K.; Xia, J. Atom Transfer Radical Polymerization. *Chem. Rev.* **2001**, *101*, 2921−2990.
(30) Grady, M. C.; Quan, C.; Soroush, M. Patent Application Number 60/484, 393, filed on July 2, 2003.
(31) Odian, G. *Principles of Polymerization*, 3rd ed.; John Wiley & Sons, Inc.: New York, 1991; pp 243−249.
(32) Stevens, M. P. *Polymer Chemistry: An Introduction*, 3rd ed.; Oxford University Press, Inc.: New York, 1999; pp 180−183.
(33) Beuermann, S.; Paquet, D. A.; McMinn, J. H.; Hutchinson, R. A. Determination of Free-Radical Propagation Rate Coefficients of Butyl, 2-Ethylhexyl, and Dodecyl Acrylates by Pulsed-Laser Polymerization. *Macromolecules* **1996**, *29*, 4206−4215.
(34) Busch, M.; Wahl, A. The Significance of Transfer Reactions in Pulsed Laser Polymerization Experiments. *Macromol. Theory Simul.* **1998**, *7*, 217−224.
(35) Nikitin, A. N.; Hutchinson, R. A.; Buback, M.; Hesse, P. Determination of Intramolecular Chain Transfer and Midchain Radical Propagation Rate Coefficients for Butyl Acrylate by Pulsed Laser Polymerization. *Macromolecules* **2007**, *40*, 8631−8641.
(36) Davis, T. P.; O'Driscoll, K. F.; Piton, M. C.; Winnik, M. A. Copolymerization Propagation Kinetics of Styrene with Alkyl Acrylates. *Polym. Int.* **1991**, *24*, 65−70.
(37) Lyons, R. A.; Hutovic, J.; Piton, M. C.; Christie, D. I.; Clay, P. A.; Manders, B. G.; Kable, S. H.; Gilbert, R. G. Pulsed-Laser Polymerization Measurements of the Propagation Rate Coefficient for Butyl Acrylate. *Macromolecules* **1996**, *29*, 1918−1927.
(38) Beuermann, S.; Buback, M. Rate Coefficients of Free-Radical Polymerization Deduced from Pulsed Laser Experiments. *Prog. Polym. Sci.* **2002**, *27*, 191−254.
(39) Yamada, B.; Azukizawa, M.; Yamazoe, H.; Hill, D. J. J.; Pomery, P. J. Free Radical Polymerization of Cyclohexyl Acrylate Involving Interconversion between Propagating and Mid-Chain Radicals. *Polymer* **2000**, *41*, 5611−5618.
(40) Farcet, C.; Belleney, J.; Charleux, B.; Pirri, R. Structural Characterization of Nitroxide-Terminated Poly(*n*-butyl acrylate) Prepared in Bulk and Miniemulsion Polymerizations. *Macromolecules* **2002**, *35*, 4912−4918.
(41) Wang, W.; Nikitin, A. N.; Hutchinson, R. A. Consideration of Macromonomer Reactins in *n*-Butyl Acrylate Free Radical Polymerization. *Macromol. Rapid Commun.* **2009**, *30*, 2022−2027.
(42) Rier, T.; Srinivasan, S.; Soroush, M.; Kalfas, G.; Grady, M. C.; Rappe, A. M. Macroscopic Mechanistic Modeling and Optimization of a Self-Initiated High-Temperature Polymerization Reactor, 2011. In *American Control Conference*, June 29−July 01, 2011, San Francisco, CA.
(43) Brandrup, A.; Immergut, E. H. In *Polymer Handbook*, 3rd ed.; Brandrup, A., Immergut, E. H., Eds.; Wiley-Inter-Science: New York, 1989.
(44) Asua, J. M.; Beuermann, S.; Buback, M.; Castignolles, P.; Charleux, B.; Gilbert, R. G.; Hutchinson, R. A.; Leiza, J. R.; Nikitin, A. N.; Vairon, J. P.; van Herk, A. M. Critically Evaluated Rate Coefficients for Free-Radical Polymerization: 5. Propagation Rate Coefficient for Butyl Acrylate. *Macromol. Chem. Phys.* **2004**, *205*, 2151−2160.
(45) Lovell, P. A.; Shah, T. H.; Heatley, F. Chain Transfer to Polymer in Emulsion Polymerization of *n*-Butyl Acrylate Studied by Carbon-13 NMR Spectroscopy and Gel Permeation Chromatography. *Polym. Commun.* **1991**, *32*, 98−103.
(46) Lovell, P. A.; Shah, T. H.; Healtley, F. In *Polymer Latexes: Preparation, Characterization and Applications*; Daniels, E. S., Sudol, E. D., E1-Asser, M., Eds.; ACS Symposium Series 492; American Chemical Society: Washington, DC, 1992; p 188.
(47) Thickett, S. C.; Gilbert, R. G. Transfer to Monomer in Styrene Free-Radical Polymerization. *Macromolecules* **2008**, *42*, 4528−4530.
(48) Srinivasan, S.; Lee, M. W.; Grady, M. C.; Soroush, M.; Rappe, A. M. Computational Evidence for Self-Initiation in Spontaneous High-Temperature Polymerization of Methyl Methacrylate. *J. Phys. Chem. A* **2011**, *115*, 1125−1132.
(49) Yu, X.; Pfaendtner, J.; Broadbelt, L. J. Ab Initio Study of Acrylate Polymerizatin Reactions: Methyl Methacrylate and Methyl Acrylate Propagation. *J. Phys. Chem. A* **2008**, *112*, 6772−6782.
(50) Bebe, S.; Yu, X.; Hutchinson, R. A.; Broadbelt, L. J. Estimation of Free Radical Polymerization Rate Coefficient Using Computational Chemistry. *Macromol. Symp.* **2006**, *243*, 179−189.
(51) Coote, M. L. Quantum-Chemical Modeling of Free-Radical Polymerization. *Macromol. Theory Simul.* **2009**, *18*, 388−400.
(52) Cohen, A. J.; Mori-Sanchez, P.; Yang, W. Insights into Current Limitations of Density Functional Theory. *Science* **2008**, *321*, 792−794.
(53) Coote, M. L. *Encyclopedia of Polymer Science and Technology*; Wiley Interscience: New York, 2006; Vol. *1*.
(54) Zhao, Y.; Truhlar, D. G. The M06 Suite of Density Functionals for Main Group Thermochemistry, Thermochemical Kinetics, Noncovalent Interactions, Excited States, and Transition Elements. *Theor. Chem. Acc.* **2008**, *120*, 215−241.
(55) Chai, J.; Head-Gordon, M. Long-Range Corrected Hybrid Density Functionals with Damped Atom Atom Dispersion Corrections. *Phys. Chem. Chem. Phys.* **2008**, *10*, 6615−6620.

(56) Hohenberg, P.; Kohn, W. Inhomogeneous Electron Gas. *Phys. Rev.* **1964**, *136*, B864−871.
(57) Wong, M. W.; Radom, L. Radical Addition to Alkenes: An Assessment of Theoretical Procedures. *J. Phys. Chem.* **1995**, *99*, 8582−8588.
(58) Van Leeuwen, R.; Baerends, E. J. Exchange-Correlation Potential with Correct Asymptotic Behavior. *Phys. Rev. A* **1994**, *49*, 2421−2431.
(59) Becke, A. D. A New Inhomogeneity Parameter in DFT. *J. Chem. Phys.* **1998**, *109*, 2092−2098.
(60) Mori-Sanchez, P.; Cohen, A. J.; Yang, W. Many-Electron Self-Interaction Error in Approximate Density Functionals. *J. Chem. Phys.* **2006**, *124*, 91102/1−91102/4.
(61) Khuong, K. S.; Jones, W. H.; Pryor, W. A.; Houk, K. N. The Mechanism of the Self-Initiated Thermal Polymerization of Styrene. Theoretical Solution of a Classic Problem. *J. Am. Chem. Soc.* **2005**, *127*, 1265−1277.
(62) Zhao, Y.; Schultz, N. E.; Truhlar, D. G. Design of Density Functionals by Combining the Method of Constraint Satisfaction with Parametrized for Thermochemistry, Thermochemical Kinetics, and Noncovalent Interactions. *J. Chem. Theory Comput.* **2006**, *2*, 364−382.
(63) Zhao, Y.; Schultz, N. E.; Truhlar, D. G. Exchange-Correlation Functionals with Broad Accuracy for Metallic and Nonmetallic Compounds, Kinetics, and Noncovalent Interactions. *J. Chem. Phys.* **2005**, *123*, 161103/1−161103/4.
(64) Zhao, Y.; Truhlar, D. G. Density Functionals with Broad Applicability in Chemistry. *Acc. Chem. Res.* **2008**, *41*, 157−167.
(65) Zhao, Y.; Truhlar, D. G. How Well Can New-Generation Density Functionals Describe the Energetics of Bond-Dissociation Reactions Producing Radicals? *J. Phys. Chem. A* **2008**, *112*, 1095−1099.
(66) Izgorodina, E. I.; Coote, M. L. Accurate *ab initio* Prediction of Propagation Rate Coefficients in Free-Radical Polymerisation: Acrylonitrile and Vinyl Chloride. *Chem. Phys.* **2006**, *324* (1), 96−110.
(67) Thickett, S. C.; Gilbert, R. G. *Polymer* **2004**, *45*, 6993−6999.
(68) Srinivasan, S. Ph.D. Thesis, Drexel University, Philadelphia, PA, 2009.
(69) PleigoJr, J. R.; Riveros, J. M. The Cluster−Continuum Model for the Calculation of the Solvation Free Energy of Ionic Species. *J. Phys. Chem. A* **2001**, *105*, 7241−7247.
(70) Warshel, A.; Levitt, M. Theoretical Studies of Enzymic Reactions: Dielectric, Electrostatic and Steric Stabilization of the Carbon Ion in the Reaction of Lysozyme. *J. Mol. Biol.* **1976**, *103*, 227−249.
(71) Vreven, T.; Morokuma, K.; Farkas, O.; Schlegel, H. B.; Frisch, M. J. Geometry Optimization with QM/MM, ONIOM, and Other Combined Methods. I. Microiterations and Constraints. *J. Comput. Chem.* **2003**, *24*, 760−769.
(72) Murphy, R. B.; Philipp, D. M.; Friesner, R. A. A Mixed Quantum Mechanics/Moleular Mechanics (QM/MM) Method for Large-Scale Modeling of Chemistry in Protein Environments. *J. Comput. Chem.* **2000**, *21*, 1442−1457.
(73) Ahmad, N. M.; Heatley, F.; Lovell, P. A. Chain Transfer to Polymer in Free-Radical Solution Polymerization of *n*-Butyl Acrylate Studied by NMR Spectroscopy. *Macromolecules* **1998**, *31*, 2822−2827.
(74) Nesse, F. *ORCA*, an ab initio, DFT, and semiempirical SCF-MO package, version 2.8.0; University of Bonn: Bonn, Germany, 2010.
(75) Wiitala, K. W.; Hoye, T. R.; Cramer, C. J. Hybrid Density Functional Methods Empirically Optimized for the Computation of ^{13}C and ^{1}H Chemical Shifts in Chloroform Solution. *J. Chem. Theory Comput.* **2006**, *2*, 1085−1092.
(76) Becke, A. D. Density-Functional Exchange-Energy Approximation with Correct Asymptotic Behavior. *Phys. Rev. A* **1988**, *38*, 3098−3100.
(77) Lee, C.; Yang, W.; Parr, R. G. Development of the Colle−Salvetti Conelation Energy Formula into a Functional of the Electron Density. *Phys. Rev. B* **1988**, *37*, 785−789.
(78) Schmidt, M. W.; Baldridge, K. K.; Boatz, J. A.; Elbert, S. T.; Gordon, M. S.; Jensen, J. H.; Koseki, S.; Matsunaga, N.; Nguyen, K. A.; Su, S. J.; Windus, T. L. The General Atomic and Molecular Electronic Structure System. *J. Comput. Chem.* **1993**, *14*, 1347−1363.
(79) Eyring, H. The Activated Complex in Chemical Reactions. *J. Chem. Phys.* **1935**, *3*, 107−115.
(80) Irikura, K. K. *THERMO.PL*; National Institute of Standards and Technology: Gaithersburg, MD, 2002.
(81) Liu, S.; Srinivasan, S.; Grady, M. C.; Soroush, M.; Rappe, A. M. Computational Study of Cyclohexanone-Monomer Co-Initiation Mechanism in Thermal Homo-Polymerization of Methyl Acrylate and Methyl Methacrylate. *J. Phys. Chem. A* **2012**, *116* (22), 5337−5348.
(82) Precomputed Vibrational Scaling Factors. http://cccbdb.nist.gov/vibscalejust.asp (accessed Feb 2012).
(83) Sanderson, R. T. *Polar Covalence*; Academic Press: New York, 1983.
(84) Jenkins, P. R.; Symons, M. C. R.; Booth, S. E.; Swain, C. J. Why is Vinyl Anion Configurationally Stable but a Vinyl Radical Configurationally Unstable? *Tetrahedron Lett.* **1992**, *33*, 3543−3546.
(85) Bond-Dissociation Energy. http://en.wikipedia.org/wiki/Bond-dissociation_energy (accessed Dec 2012).